Polymer Chemistry

ROYAL SOCIETY OF CHEMISTRY

PAPER

View Article Online
View Journal | View Issue

Open Access Article. Published on 05 May 2023. Downloaded on 1/19/2026 1:21:45 AM.
This article is licensed under a Creative Commons Attribution 3.0 Unported Licence.

Check for updates

Cite this: *Polym. Chem.*, 2023, **14**, 2734

Post-polymerisation modification of poly(3-hydroxybutyrate) (PHB) using thiol–ene and phosphine addition†

Lucas Al-Shok, James S. Town, Despina Coursari, Paul Wilson and David M. Haddleton *

As we face the issues associated with fossil resource-based polymers and their environmental impact after their useful life, polyesters become more important as "greener" alternatives due to their potential hydrolytic and enzymatic degradability in various environments. Moreover, post-modifying their structure can additionally open up access to a variety of new materials. During this work the potential to post-modifying synthetic PHB made *via* the organocatalysed ring-opening polymerisation of β-butyrolactone (β-BL) is shown. Modification by thiol–ene 'click' chemistry was succesfully conducted under UV-initiation. Surprisingly, attempting the modification under thermal conditions using dimethylphenylphosphine (DMPP) as catalyst, resulted in the attachment of the phosphine, as shown *via* NMR spectroscopy. Control experiments using crotonic acid, methyl crotonate and *n*-butyric acid indicated that the presence of a carboxylic acid group is necessary in order for the phosphine addition to occur. Further, the formation of particles shown *via* dynamic light scattering (DLS), zeta-potential (ZP) and transmission electron microscopy (TEM) measurements suggest an amphiphilic character of the phosphine-functionalised polymers. Finally, stability studies in the presence of salt and different pH environments revealed a high responsiveness and dependency between pH and particle size as well as surface charge.

Received 14th March 2023,
Accepted 4th May 2023

DOI: 10.1039/d3py00272a

rsc.li/polymers

1. Introduction

Poly(3-hydroxybutyrate) (PHB) is a high molecular weight thermoplastic polymer produced by microorganisms[2,3] and has been used as a thermoplastic from a renewable route, which biodegrades under ambient and mild conditions.[4–8] However, highly crystalline natural occurring PHB exhibits low thermostability and hence unfavourable properties for melt processing. Therefore, various synthetic routes of producing PHB designed to circumvent the high production costs are subject of ongoing research efforts.[9–12]

Producing synthetic PHB paves the way for influencing the properties by changing reaction conditions and the resulting polymeric structure. Introducing functionality into a polymer is of great interest to widen the prospects for different applications either by using a functional monomer or initiator design.[13–20] Another widely used approach is the modification of end groups after polymerisation.[19,21] Jaffredo *et al.* reported the organocatalysed ring-opening polymerisation (ROP) of β-butyrolactone (β-BL) resulting in PHB exhibiting a crotonyl functionality as α-end group.[1,14,22] In 2018 Coulembier expanded this work and postulated a mechanism for the ROP of β-BL catalysed by 1,5,7-triazabicyclo[4.4.0]dec-5-ene (TBD) involving an intermediate of protonated TBD and crotonate. The crotonate is acting as the polymerisation initiator selectively opening β-BL *via* a *O*-alkyl cleavage.[23] These crotonate functionalities yield the potential for post-polymerisation modification. As shown by Michalak *et al.*, successful epoxidation of crotonate functionalities can be achieved by using *m*CPBA followed by reacting the epoxide with alcohols and amines, respectively.[24] In a follow-up study, the authors could further show the functionalisation of the crotonate end group by ozonolysis resulting in glyoxylate-end capped PHB, which could be used for designing potential biocompatible drug delivery systems.[25]

Moreover, thiol–ene "click chemistry" has been used to functionalise vinyl and the less reactive crotonyl groups.[26] Yu and co-workers investigated the post-polymerisation modification of both allylic side chains and crotonic end groups of poly(4-allyloxymethyl-β-propiolactone).[27]

Further, phosphines can be regarded as potentially interesting reaction partners for crotonates as they participate in Michael-addition reactions and are commonly used as catalysts.[28,29] Galkin and co-workers reported on the functionalisation of unsaturated carboxylic acids using phosphines.[30–34]

Department of Chemistry University of Warwick, Library Road, CV4 7AL Coventry, UK. E-mail: d.m.haddleton@warwick.ac.uk

† Electronic supplementary information (ESI) available. See DOI: https://doi.org/10.1039/d3py00272a

This journal is © The Royal Society of Chemistry 2023

Open Access Article. Published on 05 May 2023. Downloaded on 1/19/2026 1:21:45 AM.
This article is licensed under a Creative Commons Attribution 3.0 Unported Licence.

In particular, Bu_3P has been described to form an irreversible acid-phosphine adduct.

The prospect of this study is to contribute to the ongoing investigation of the post-polymerisation modification of crotonate-end capped synthetic PHB and to elaborate on the potential property modifications of the atactic and amorphous material. Polymers with relatively low molecular weights (>7000 g mol^{-1}) have been synthesised to make the effect of the modified end group functionality on the polymer properties apparent. In addition to thiol–ene chemistry, the crotonate functionality could be modified by using phosphines, which unexpectedly resulted in amphiphilic properties and aggregating structures.

2. Experimental

2.1 Raw materials

β-Butyrolactone was stirred and vacuum-distilled over CaH_2 and stored in a flame-dried Schlenk tube over molecular sieves under nitrogen. If not otherwise stated, all chemicals were purchased from commercial vendors, including Sigma-Aldrich, Thermo Fisher Scientific and Alfa Aesar.

2.2 Synthesis of poly(3-hydroxybutyrate)

In a general procedure, 1–4 mol% TBD was added to a flame dried Schlenk tube. 1 mL of β-BL was added under stirring *via* a gas-tight syringe under a nitrogen atmosphere. The reaction was stirred at 60 °C and quenched by the addition of dichloromethane. The polymer solution was then stirred over ion-exchange resin Amberlite IR-120(H) to remove TBD. PHB was precipitated into cold *n*-pentane three times before being isolated by the removal of volatiles under vacuum at 40 °C for 24 h (Scheme 1).

^{1}H NMR (400 MHz, $CDCl_3$) δ [ppm] 6.96 (m, J = 6.5 Hz, CH, 1H), 5.83–5.79 (d, J = 15.5 Hz, CH, 1H), 5.26 (m, CH, backbone), 2.64–2.44 (m, CH_2, backbone), 1.88–1.87 (d, J = 6.8 Hz, CH_3, 3H), 1.28 (m, CH_3, backbone).

2.3 Post-polymerisation modification: thiol–ene

In a glass vial, PHB (1300 g mol^{-1}, 0.08 mmol) was dissolved in 3 mL $CDCl_3$ before 2,2-dimethoxy-2-phenylacetophenone (DMPA) (1.1 eq., 0.185 mmol) were added to the solution. Subsequently, methylthioglycolate (MTG) (10 eq., 1.68 mmol) was added dropwise to the mixture. After deoxygenated by bubbling with nitrogen for 20 minutes the vial was irradiated by UV light (λ = 365 nm, 500 mJ cm^{-3}) over night. The functionalised polymer was precipitated into *n*-pentane three time and all volatiles were removed under vacuum. The completion of the reaction was validated by monitoring the crotonyl-peaks (6.96 and 5.83 ppm) in the ^{1}H-NMR.

2.4 Post-polymerisation modification: phosphine

In a glass vial, PHB (1000 g mol^{-1}, 0.1 mmol) was dissolved in 2 mL of $CDCl_3$ and deoxygenated for 20 minutes. Afterwards, DMPP (5 eq., 0.42 mmol) was added to the solution before increasing the temperature of the reaction mixture to 50 °C. The reaction was stirred overnight and quenched by removing it from the heat source. All volatiles were removed under vacuum. The completion of the reaction was validated by monitoring the crotonyl-peaks (6.96 and 5.83 ppm) in the ^{1}H-NMR. The functionalised polymer was purified *via* multiple precipitations into diethyl ether and drying under air. The reaction with Bu_3P was conducted accordingly.

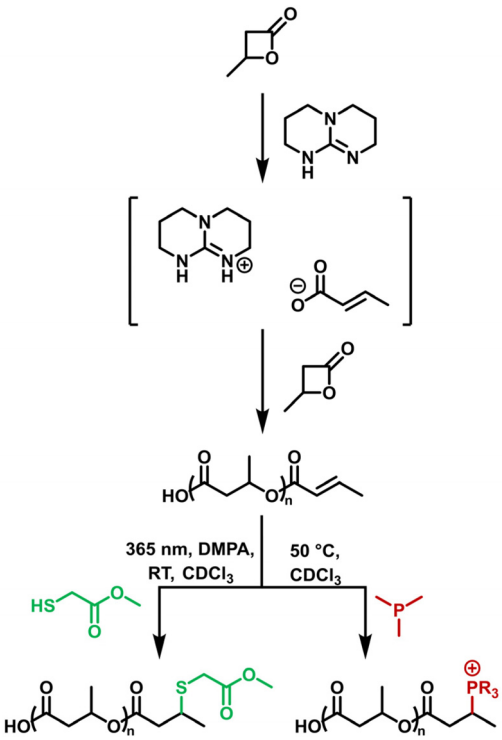

Scheme 1 Polymerisation of β-butyrolactone using TBD as the organocatalyst results in PHB end-capped with a crotonyl functionality. The crotonyl group can be further functionalised *via* thiol–ene 'click' chemistry (**green**) using UV conditions and DMPA as initiator or by attaching a phosphine (**red**) *via* thermal activation.

2.5 Post-polymerisation modification: control experiments

In a glass vial, either methyl-crotonate (1 mmol), crotonic acid (0.85 mmol) or *n*-butyric acid (0.84 mmol) was dissolved in 2 mL of $CDCl_3$, deoxygenated for 20 minutes, mixed with DMPP (5 eq., 5 mmol), immersed at 50 °C and stirred overnight. The reaction was quenched by removing the heat source and all volatiles were removed under vacuum. The reaction was monitored by using ^{1}H and ^{31}P-NMR.

2.6 Stability studies

As PHB can be prone to hydrolysing in acidic and basic environments, unfunctionalised PHB and low molecular weight PHB-DMPP were suspended in 0.9 wt% acidic and basic buffer, respectively. On the next day the samples were freeze-dried and investigated *via* ^{1}H-NMR.

Open Access Article. Published on 05 May 2023. Downloaded on 1/19/2026 1:21:45 AM. This article is licensed under a Creative Commons Attribution 3.0 Unported Licence.

2.7 Characterisation

2.7.1. Solution nuclear magnetic resonance (NMR) spectroscopy. Solution nuclear magnetic resonance (NMR) spectroscopy were recorded on either a Bruker DPX-300 or a Bruker DPX-400 MHz instrument, using deuterated chloroform ($CDCl_3$) or deuterated dimethyl sulfoxide (DMSO-d_6) as solvents. Chemical shifts are given as δ in parts per million (ppm) downfield from the internal standard tetramethylsilane (TMS) at δ = 0 ppm. ^{31}P-NMR spectra were recorded with ^{1}H-decoupling at 161 MHz. Monomer conversion was calculated by comparison of the CH of lactone (4.67–4.60 ppm) with CH protons (5.26 ppm) of PHB. All spectra were analysed using ACD/NMR processor or MestReNova software.

2.7.2 Size exclusion chromatography (SEC). SEC were recorded on an Agilent Infinity II MDS instrument equipped with differential refractive index (DRI). The system was equipped with 2 × PLgel mixed C columns (300 × 7.5 mm) and a PLgel 5 μm guard column (or a single mixed E column). The eluent used was THF with 0.01% BHT (butylated hydroxytoluene) additives. Samples were run at 1 ml min^{-1} at 30 °C. Analyte samples were filtered through a nylon membrane with 0.22 μm pore size before injection. Experimental molar mass (M_n) and dispersity ($Đ$) of synthesised polymers were determined by conventional calibration using narrow molecular weight poly(methyl methacrylate) (11 narrow standards between 2 210 000–1010 Da) and polystyrene standards (12 narrow standards between 364 000–160 Da (Agilent EasiVials) with Agilent GPC/SEC software.

2.7.3 Matrix-assisted laser-desorption ionisation time of flight (MALDI-ToF) spectrometry. Samples of the homopolymers were prepared in $CHCl_3$ or THF at a concentration of 10 mg mL^{-1}, with the addition of 1 mg mL^{-1} of NaI or KI as a cationising agent. PEG (calibration standards) was prepared in THF at a concentration of 10 mg mL^{-1}, with an addition of 1 mg mL^{-1} of NaI or KI as a cationising agent. All samples were subsequently mixed 1 : 1 with a 40 mg mL^{-1} solution of *trans*-2-[3-(4-*tert*-butylphenyl)-2-methyl-2-propenylidene] malononitrile (DCTB) in THF. PHB samples were mixed 1 : 1 with a 40 mg mL^{-1} solution of super-dihydroxybenzoic acid (sDHB, 9 : 1 (w/w) mixture of 2,5-DHB and 2-hydroxy-5-methoxybenzoic acid). The samples, 0.5 μL of each, were then spotted on an MTP 384 ground steel target plate and analysed using a Bruker AutoFlex speed ToF/ToF analyser, equipped with a 337 nm nitrogen laser.

2.7.4 Fluorescence spectroscopy. Fluorescence spectroscopy measurements were taken on a Cary Eclipse fluorescence spectrophotometer at ambient temperature. Solutions of the DMPP-functionalised polymer in various concentrations were made up in deionized water *via* serial dilutions. A stock solution of pyrene (2.5 × 10^{-4} M) was made in filtered acetone (0.45 μm pores size). 12 μL of the stock solution were added to empty vials and the acetone was left to evaporate under air for 2 h before the polymer solutions were added to make up the samples with the final pyrene concentration of 6 × 10^{-7} M. Excitation spectra were recorder from λ = 300 nm to 360 nm with the emission wavelength at λ = 394 nm and a scan rate of 600 nm min^{-1}. Intensities of λ = 333 nm and 338 nm were compared.

2.7.5 Dynamic light scattering (DLS). Dynamic light scattering (DLS) measurements were carried out on an Anton-Paar Litesizer 500. All size measurements were made using samples of concentrations of 1 mg mL^{-1} in either deionised filtered water (0.45 μm pore size), or salt and buffer solutions with 0.9 and 0.09 wt% salt content at 25 °C, with light scattering detected at an angle of 175° (back-scattering). All samples were filtered through a 0.45 μm syringe filter and the cuvette was rinsed with deionised water three times, to minimize dust contamination. Hydrodynamic diameters (D_h) were determined from correlograms using the cumulant model. Diffusion coefficients were calculated *via* the Stokes–Einstein equation, which assumes perfectly monodisperse non-interacting spheres and averaged over 5 consecutive runs with at least 60 measurements recorded for each run. PEtOx was used as a material reference. For salt and pH dependent measurements, samples were prepared in NaCl and buffer solutions with concentrations of 0.9 or 0.09 wt%, respectively.

2.7.6 ZETA-potential. ZETA-potential measurements were conducted on an Anton-Paar Litesizer 500 using an Omega cuvette (mat. no. 225288) and sample concentrations of 1 mg mL^{-1} in deionised filtered water (0.45 μm pore size) or salt and buffer solutions with 0.9 and 0.09 wt% salt content at 25 °C. The measurement was taken with an adjusted voltage of 200 V. The measured zeta-potential was averaged over 5 consecutive runs with 100 measurements recorded. For salt and pH dependent measurements, samples were prepared in NaCl and buffer solutions (pH 4, 7 and 9) with concentrations of 0.9 or 0.09 wt%, respectively.

2.7.7 Transmission electron microscopy (TEM). Transmission electron microscopy (TEM) was carried out on a Jeol 2100, fitted with a Gatan Ultrascan 1000 camera at 200 kV acceleration voltage. A solution of polymer was prepared with a concentration of 1 mg mL^{-1}. A drop from that solution was left on a grid (formvar/carbon coated copper) to dry for 1 min. The residual solution was blotted away with filter paper. The grid was then stored at room temperature until imaging. Particle sizes were determined form an average of 20 particles using ImageJ software.

3. Results and discussion

3.1 Synthesis of poly(3-hydroxybutyrate)

PHB with molecular weights between 1000 and 5300 g mol^{-1} were synthesised by the reaction of β-BL with TBD in a flame-dried Schlenk tube overnight at 60 °C, according to the procedure described by Jaffredo.[1] Molecular weight was determined using ^{1}H-NMR with the chemical shifts at 5.7 ppm and 6.9 ppm as an indication of the crotonate end group (Fig. S5–S8†). MALDI-ToF MS confirmed the presence of both the crotonate and acid α, ω terminal groups of PHB (Fig. S10–S13†).

 This journal is © The Royal Society of Chemistry 2023

Open Access Article. Published on 05 May 2023. Downloaded on 1/19/2026 1:21:45 AM.
This article is licensed under a Creative Commons Attribution 3.0 Unported Licence.

3.2 Post-polymerisation modification

3.2.1 UV-initiated thiol–ene. Post-polymerisation modification was carried out by utilising the crotonate end group generated through the TBD-catalysed ROP pathway of PHB. The end group was functionalised *via* reaction of the crotonate using the photo-induced thiol–ene reaction of methyl thioglycolate (MTG), with 2,2-dimethoxy-2-phenylacetophenone (DMPA) as the initiator. The disappearance of the proton signals from the crotonate and detection of the end groups *via* MALDI-ToF MS suggests a successful reaction (Fig. 1 and S21†).

3.2.2 Phosphine addition. Thiol–ene functionalisation was also attempted *via* nucleophilic activation using DMPP as catalyst. Surprisingly, the MALDI-ToF spectra of the functionalised polymers showed identical signals independent from the thiol used. These signals could be assigned as [polymer-DMPP] adducts with DMPP acting as a counter ion (Fig. 2 and S26, S35 and S44†). Thus, to distinguish between a MALDI-specific phenomenon and a possible covalent attachment of the phosphine during the reaction further NMR studies were required. A comparison of the ^{31}P NMR spectra of DMPP and functionalised polymer showed a significant shift of the signal from −45 ppm (DMPP) to 22, 31 and 34 ppm, which could be attributed to a structural change of the phosphine (Fig. S15, S23, S32 and S41†). The peak at 34 ppm suggests that DMPP oxide is formed as a by-product.[35] In addition, diffusion-ordered spectroscopy (DOSY) (Fig. 3a) and ^{1}H–^{31}P correlation NMR (Fig. 3b) allowed for the assignment of the chemical shift at 31 ppm to a functionalised PHB species with covalently bound DMPP. When the experiments were repeated with different phosphines (Ph_3P, $cyHex_3P$, Bu_3P), Bu_3P also resulted in disappearance of crotonate signals in the ^{1}H-NMR and a shift in the ^{31}P-NMR (Fig. S17, S25, S34 and S43†), whereas Ph_3P and $cyHex_3P$ didn't seem to react with the crotonate functionality. It is noted that DMPP and Bu_3P have a comparably low cone angle of 122° and 132°, respectively.[36,37] Thus, decreased steric hindrance seems to favour this reaction.

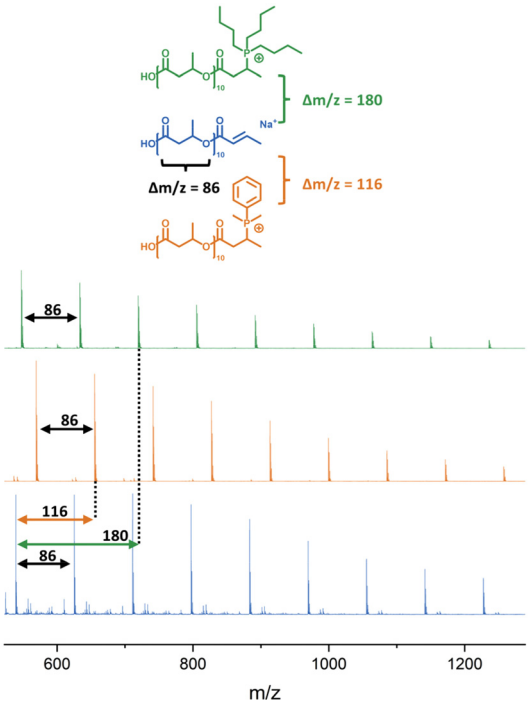

Fig. 1 (a) ^{1}H-NMR after thiol–ene functionalisation of low molecular weight PHB with MTG. (b) MALDI-ToF MS of functionalised PHB-MTG showing sodium adducts.

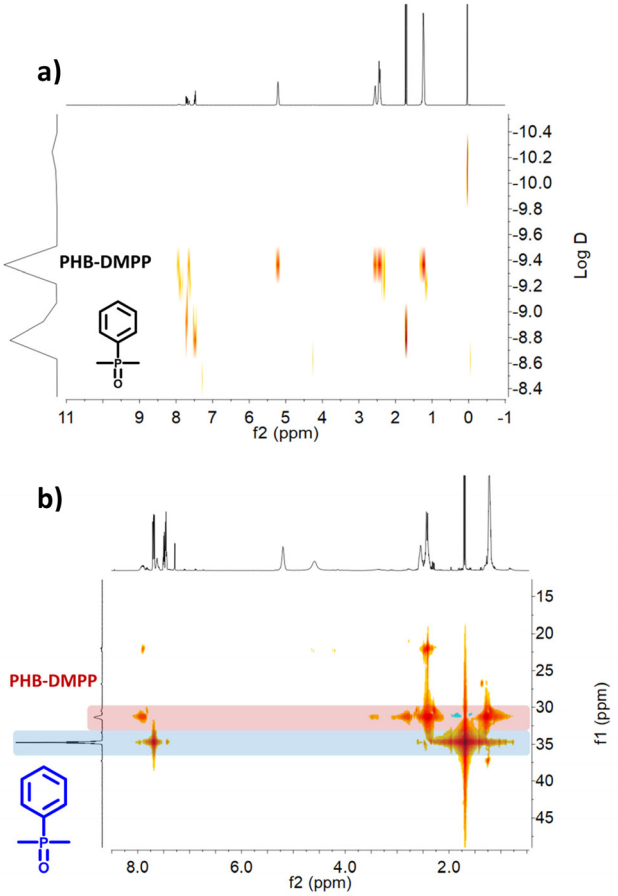

Fig. 2 MALDI-ToF spectra of unfunctionalised (uf) PHB compared to PHB functionalised with DMPP and Bu_3P, respectively.

3.2.3 Structural elucidation of phosphine functionalisation. In order to determine the structure of the polymer adduct several control experiments using small molecules like *n*-butyric acid, methyl-crotonate and crotonic acid were conducted. Only crotonic acid displayed a significant shift in the ^{31}P NMR and ^{1}H–^{31}P NMR correlation after reaction with both DMPP and Bu_3P (Fig. S49–S53†). Moreover, the proton-signal corresponding to the CH_3 changed its splitting pattern from a doublet to a doublet of doublets (Fig. 4) suggesting coupling to a proton and phosphorous nucleus bonded to the carbon adjacent to the CH_3.

Reaction with a mixture of methyl-crotonate and *n*-butyric acid in the presence of DMPP or Bu_3P gave a similar functiona-

Open Access Article. Published on 05 May 2023. Downloaded on 1/19/2026 1:21:45 AM.
This article is licensed under a Creative Commons Attribution 3.0 Unported Licence.

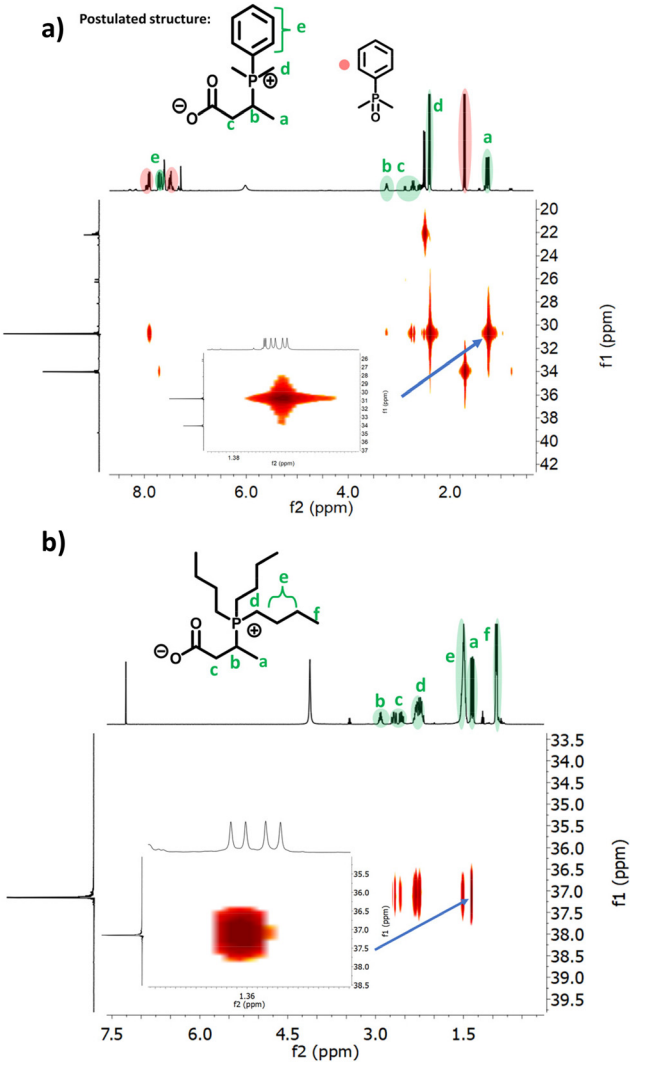

Fig. 3 (a) DOSY-NMR of DMPP-functionalised PHB. (b) $^{1}H-^{31}P$ correlation NMR of DMPP-functionalised PHB showing phosphine oxide (blue) and functionalised polymer (red).

lisation to the crotonic acid and PHB phosphine additions (Fig. S54–S57†), suggesting the successful functionalisation of methyl-crotonate. Thus, in order for the double bond functionalisation to happen, an additional acid group is required. Interestingly, for crotonic acid the signal of the carboxylic acid shifts from 12 ppm to 6 ppm, indicating a less acidic proton or an interaction between the carbonyl-oxygen and the neighbouring phosphorous. A similar shift was also observed for the mixture of *n*-butyric acid and methyl-crotonate, suggesting a similar O–P interaction. Alternatively, the residual peak at 6 ppm could corresponds to complexed water.

Repeating the NMR measurement in DMSO resulted in a significant shift toward higher field (3.4 ppm) agreeing with a residual water signal. Galkin *et al.* described a mechanism of their 'phosphabetaine' formation, involving the deprotonation of the carboxylic acid and the identification of water incorporated in the crystal lattice which supports this explanation.[32]

a)

	PHB-DMPP				PHB-Bu_3P			
Molecular weight $[g/mol]_{NMR}$	1000	1300	2000	5300	1000	1300	2000	5300
CAC [mg/mL]	0.123	0.052	0.021	0.048	0.075	0.015	0.011	0.083
D_H [nm] (PDI)	210 ± 63 (0.13)	139 ± 62 (0.22)	130 ± 38 (0.14)	269 ± 76 (0.26)	187 ± 50 (0.12)	222 ± 120 (0.25)	272 ± 128 (0.25)	236 ± 69 (0.27)
ZP	48	56	58	67	12	44	65	68
PD_{TEM} [nm]	218 ± 81	93 ± 15	173 ± 25	279 ± 54	228 ± 95	251 ± 53	247 ± 40	97 ± 24

b)

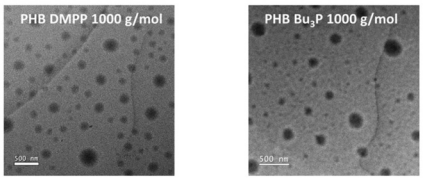

Fig. 4 ^{1}H (f2)–^{31}P (f1) NMR correlation spectrum of functionalised crotonic acid using DMPP (a) and Bu_3P (b), respectively. Signals labelled with a red background correspond to oxidised phosphine, a green background refers to functionalised crotonic acid. The insert shows the resolved splitting pattern of the methyl group showing a characteristic doublet–doublet splitting and therefore suggesting coupling to an adjacent phosphorous.

3.3 Self-assembly of functionalised PHB

The phosphine-modification of PHB using DMPP and Bu_3P resulted in an amphiphilic molecule, which became evident by observing the formation of dispersions in aqueous media after functionalisation. In contrast, unfunctionalised PHB precipitates in aqueous media and forms visible sedimentation.

PHB with molecular weights between 1000 and 5300 g mol^{-1} were functionalised using both Bu_3P and DMPP. Following the determination of the critical aggregation concentration (CAC), the particles were characterised *via* zeta-potential (ZP) measurements, DLS and TEM (Fig. 5). Functionalised PHB-DMPP with a molecular weight of 1000 g mol^{-1} gave a CAC of 0.12 mg mL^{-1} observed *via* fluorescence of pyrene in the presence of different concentrations of functionalised polymer (Fig. S18, S27, S36 and S45†).[38] In comparison, sodium dodecyl sulphate (SDS), which is commonly used as surfactant additive typically shows a CAC of 0.008 mol L^{-1} (2.3 mg mL^{-1}) in aqueous media.[39] This would be several magnitudes higher than the measured CAC for

a)

	PHB-DMPP				PHB-Bu_3P			
Molecular weight $[g/mol]_{NMR}$	1000	1300	2000	5300	1000	1300	2000	5300
CAC [mg/mL]	0.123	0.052	0.021	0.048	0.075	0.015	0.011	0.083
D_H [nm] (PDI)	210 ± 63 (0.13)	139 ± 62 (0.22)	130 ± 38 (0.14)	269 ± 76 (0.26)	187 ± 50 (0.12)	222 ± 120 (0.25)	272 ± 128 (0.25)	236 ± 69 (0.27)
ZP	48	56	58	67	12	44	65	68
PD_{TEM} [nm]	218 ± 81	93 ± 15	173 ± 25	279 ± 54	228 ± 95	251 ± 53	247 ± 40	97 ± 24

b)

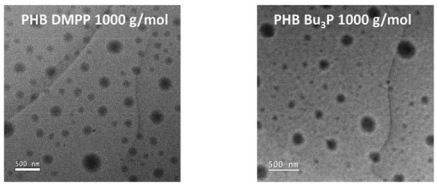

Fig. 5 (a) Table summarising observed CAC, D_h, ZP and particle diameters (PD) for PHB functionalised with DMPP or Bu_3P, respectively. Molecular weights were determined by ^{1}H-NMR. (b) TEM pictures taken from the low molecular weight PHB functionalised with DMPP or Bu_3P.

 This journal is © The Royal Society of Chemistry 2023

Open Access Article. Published on 05 May 2023. Downloaded on 1/19/2026 1:21:45 AM.
This article is licensed under a Creative Commons Attribution 3.0 Unported Licence.

Table 1 Summary of measured D_h and zeta-potential for low molecular weight PHB-DMPP and PHB Bu_3P in different salt and buffer solutions and concentrations. Green indicating stable particles, yellow initially stable particles with observed sedimentation after 1 h and red unstable particles which showed immediate sedimentation

	DIW	NaCl		pH 4		pH 7		pH 9	
PHB-DMPP low MW									
Salt wt%		0.9	0.09	0.9	0.09	0.9	0.09	0.9	0.09
D_h [nm]	211 ± 25	N/A	281 ± 117	N/A	N/A	N/A	263 ± 82	176 ± 39	197 ± 58
PDI	0.13		0.22				0.24	0.07	0.14
ZP [mV]	49	13	14	−4	13	−20	−26	−35	−49
PHB-Bu_3P low MW									
Salt wt%		0.9	0.09	0.9	0.09	0.9	0.09	0.9	0.09
D_h [nm]	187 ± 50	N/A	212 ± 42	241 ± 53	N/A	319 ± 150	290 ± 66	189 ± 95	117 ± 58
PDI	0.12		0.18	0.20		0.26	0.10	0.24	0.23
ZP [mV]	37	−10	−6	−5	−5	−19	−29	−42	−60

any phosphine-functionalised PHB, which showcases the effectiveness as potential surfactants.

ZP measurements (Fig. S19, S28, S37 and S46†) of unfunctionalised and functionalised polymer showed a significant difference of the precursor PHB with ZPs between −67 and −20 mV, PHB-DMPP with a positive ZP between 49–67 mV and PHB-Bu_3P with 37–68 mV.

DLS measurements (Fig. S20, S29, S38 and S47†) provided further evidence that the functionalised polymers formed particles with aggregates of 130–269 nm (PHB-DMPP) and 187–272 nm (PHB-Bu_3P). Dry-state transmission electron microscopy (TEM) showed particles with comparable diameters between 93 and 279 nm (Fig. 5b and S30, S39, S48†). In general, the large size of particles possibly suggests a form of self-assembly or ordered stacking of multiple chains, possibly facilitated by a positively charged phosphine and a negatively charged carboxylate end group.

The particle size distributions (PDI) for the functionalised particles lie between 0.12 and 0.27, showing stable particles with moderately broad dispersity. In particular, low molecular weight conjugates show narrower distributions, which suggests higher stability at low molecular weight.

3.4 Self-assembly as a function of salt and pH

In order to elaborate on the presumably charged surface of the dispersed particles, further stability studies were conducted by investigating the aggregation behaviour of low molecular weight PHB-DMPP and PHB-Bu_3P in different salt and buffer solutions testing the influence of salt concentration and pH, respectively (Table 1).

In comparison to aggregates formed in deionised water, NaCl solutions (Fig. S57–S59†) with 0.9 wt% (physiological concentration) showed immediate sedimentation suggesting a disruption of particles by blocking the charged sites with counter ions. Decreasing the NaCl-concentration 10-fold resulted in relatively large particles for PHB-DMPP (281 nm) and PHB-Bu_3P (212 nm) with PDI's of 0.22 and 0.18, respectively. A decrease in ZP compared to deionised water suggests a decreased surface charge due to interactions with counter ions. Notably, PHB-DMPP seemed to form particles at 0.09 wt% NaCl with a positive ZP of 14 mV in contrast to the negative −6 mV of PHB-Bu_3P, possibly due to less prominent salt interactions of PHB-DMPP. Interestingly, sedimentation was observed for 0.09 wt% NaCl suspensions of PHB-DMPP and PHB-Bu_3P after 1 h, which would be indicative for decreased stability over time.

Testing the aggregation in dependence of pH 4 (Fig. S61–S63†), pH 7 (Fig. S64–S67†) and pH 9 (Fig. S68–S71†) revealed no aggregation in pH 4 irrespective of concentration and phosphine functionality. Taking in to account the pK_a values of both cotonic acid (4.6),[40] DMPP (6.5)[41] and Bu_3P (8.4)[42] provides an estimation that both functionalised polymers could bear protonated end groups at pH 4 and are therefore not able to form suspended particles.

For pH 7 the most distinct differences between PHB-DMPP and PHB-Bu_3P can be observed. At 0.9 wt%, PHB-Bu_3P forms aggregates with an increased D_h compared to deionised water, whereas PHB-DMPP shows immediate sedimentation. However, upon decreasing the salt concentration to 0.09 wt% the D_h for PHB-Bu_3P is comparable to the prior, while PHB-DMPP forms measurable particles with similar diameters. This different behaviour toward salt concentration could highlight the sensitive aggregation of PHB-DMPP close to the pK_a of the phosphine.

At basic pH both PHB-DMPP and PHB-Bu_3P show similar stable aggregation and particle sizes compared to deionised water. The ZP shows an even strong shift toward negative values (−35 to −60 mV) compared to neutral pH which could be caused by an increased number of anions associated with the particle surface.

^{1}H-NMR were recorded for PHB before and after being kept in acidic and basic buffer, respectively. Neither unfunctionalised nor functionalised PHB showed detectable degradation products after the treatment (Fig. S72 and S73†), suggesting minimal hydrolysation in 0.9 wt% acidic and basic buffer.

4 Conclusion

In this work we have demonstrated the successful post-polymerisation modification of synthetic PHB from TBD-catalysed

Open Access Article. Published on 05 May 2023. Downloaded on 1/19/2026 1:21:45 AM.
This article is licensed under a Creative Commons Attribution 3.0 Unported Licence.

ROP of β-BL. The resulting crotonate end group could be functionalised under conventional UV-mediated thiol–ene conditions. However, when conducted under thermal conditions, the double bond was functionalised with the used phosphine catalyst (DMPP). The structure of the product was determined *via* ^{1}H-, ^{31}P-, DOSY- and ^{1}H–^{31}P-NMR correlation experiments. A carboxylic acid is required for this reaction to occur, as has been shown with control experiments where methyl-crotonate could only be functionalised in the presence of *n*-butyric acid. In order to investigate the self-assembly behaviour, polymers with molecular weights between 1000 and 5300 g mol^{-1} were synthesised and subsequently functionalised with DMPP and Bu_3P, respectively. DLS and TEM measurements showed stable aggregates with diameters between 100 and 300 nm, suggesting an intermolecular aggregation process resulting in self-assembled structures. However, at higher molecular weights, hydrophobic interactions seem to dominate and cause random aggregation. Further, stability studies in different salt concentrations and pH environments revealed high stability in alkaline pH, good to low stability in pH 7 and low stability in pH 4 as well as physiological concentrations of NaCl. These results highlight the importance of the role of the charged end groups of the functionalised polymers and how the stability can be influenced by the environment.

Conflicts of interest

There are no conflicts to declare.

Acknowledgements

L. Al-Shok thanks the University of Warwick for a PhD studentship through the Warwick Centre for Doctoral Training in Analytical Science. We thank the Research Technology Platforms (RTP) of the University of Warwick and Dr Daniel Lester for providing training and equipment and EPSRC for equipment funded in part by EPSRC EP/V036211/1 and EP/V007688/1.

References

1 C. G. Jaffredo, J. F. Carpentier and S. M. Guillaume, *Macromol. Rapid Commun.*, 2012, **33**, 1938.
2 R. W. Lenz and R. H. Marchessault, *Biomacromolecules*, 2005, **6**, 1.
3 Y. Poirier, D. Dennis, K. Klomparens, C. Nawrath and C. Somerville, *FEMS Microbiol. Lett.*, 1992, **103**, 237.
4 W. J. Orts, G. A. R. Nobes, J. Kawada, S. Nguyen, G.-E. Yu and F. Ravenelle, *Can. J. Chem.*, 2008, **86**, 628.
5 J. Mergaert, A. Webb, C. Anderson, A. Wouters and J. Swings, *Appl. Environ. Microbiol.*, 1993, **59**, 3233.
6 L. Savenkova, Z. Gercberga, O. Muter, V. Nikolaeva, A. Dzene and V. Tupureina, *Process Biochem.*, 2002, **37**, 719.
7 L. Savenkova, Z. Gercberga, V. Nikolaeva, A. Dzene, I. Bibers and M. Kalnin, *Process Biochem.*, 2000, **35**, 573.
8 M. P. Arrieta, J. López, E. Rayón and A. Jiménez, *Polym. Degrad. Stab.*, 2014, **108**, 307.
9 C. M. Thomas, *Chem. Soc. Rev.*, 2010, **39**, 165.
10 R. M. Shakaroun, P. Jéhan, A. Alaaeddine, J.-F. Carpentier and S. M. Guillaume, *Polym. Chem.*, 2020, **11**, 2640.
11 J.-F. Carpentier, *Macromol. Rapid Commun.*, 2010, **31**, 1696.
12 Z. Jedlinski, P. Kurcok and R. W. Lenz, *Macromolecules*, 1998, **31**, 6718.
13 C. G. Jaffredo and S. M. Guillaume, *Polym. Chem.*, 2014, **5**, 4168.
14 C. G. Jaffredo, J.-F. Carpentier and S. M. Guillaume, *Polym. Chem.*, 2013, **4**, 3837.
15 M. Helou, G. Moriceau, Z. W. Huang, S. Cammas-Marion and S. M. Guillaume, *Polym. Chem.*, 2011, **2**, 840.
16 C. Guillaume, N. Ajellal, J.-F. Carpentier and S. M. Guillaume, *J. Polym. Sci., Part A: Polym. Chem.*, 2011, **49**, 907.
17 R. J. Pounder and A. P. Dove, *Polym. Chem.*, 2010, **1**, 260.
18 C. K. Williams, *Chem. Soc. Rev.*, 2007, **36**, 1573.
19 S. M. Guillaume, *Eur. Polym. J.*, 2013, **49**, 768.
20 D. Kai, K. Zhang, S. S. Liow and X. J. Loh, *ACS Appl. Bio Mater.*, 2019, **2**, 127.
21 T. Ouchi, T. Uchida, H. Arimura and Y. Ohya, *Biomacromolecules*, 2003, **4**, 477.
22 C. G. Jaffredo, J.-F. Carpentier and S. M. Guillaume, *Macromolecules*, 2013, **46**, 6765.
23 S. Moins, C. Henoumont, J. De Winter, A. Khalil, S. Laurent, S. Cammas-Marion and O. Coulembier, *Polym. Chem.*, 2018, **9**, 1840.
24 M. Michalak, M. Kawalec and P. Kurcok, *Polym. Degrad. Stab.*, 2012, **97**, 1861.
25 M. Michalak, A. A. Marek, J. Zawadiak, M. Kawalec and P. Kurcok, *Eur. Polym. J.*, 2013, **49**, 4149.
26 J. W. Chan, C. E. Hoyle, A. B. Lowe and M. Bowman, *Macromolecules*, 2010, **43**, 6381.
27 Y. Yu, M. Kim, G. S. Lee, H. W. Lee, J. G. Kim and B.-S. Kim, *Macromolecules*, 2021, **54**, 10903.
28 D. H. Valentine Jr. and J. H. Hillhouse, *Synthesis*, 2003, 317.
29 C. Gimbert, M. Lumbierres, C. Marchi, M. Moreno-Mañas, R. M. Sebastián and A. Vallribera, *Tetrahedron*, 2005, **61**, 8598.
30 Y. V. Bakhtiyarova, R. R. Minnullin, I. V. Galkina, R. A. Cherkasov and V. I. Galkin, *Russ. J. Gen. Chem.*, 2015, **85**, 2037.
31 V. I. Galkin, A. V. Salin, Y. V. Bakhtiyarova and A. A. Sobanov, *Russ. J. Gen. Chem.*, 2009, **79**, 919.
32 V. I. Galkin, Y. V. Bakhtiyarova, R. I. Sagdieva, I. V. Galkina and R. A. Cherkasov, *Heteroat. Chem.*, 2006, **17**, 557.
33 V. I. Galkin, Y. V. Bakhtiyarova, N. A. Polezhaeva, I. V. Galkina, R. A. Cherkasov, D. B. Krivolapov, A. T. Gubaidullin and I. A. Litvinov, *Russ. J. Gen. Chem.*, 2002, **72**, 376.

 This journal is © The Royal Society of Chemistry 2023

Open Access Article. Published on 05 May 2023. Downloaded on 1/19/2026 1:21:45 AM.
This article is licensed under a Creative Commons Attribution 3.0 Unported Licence.

34 V. I. Galkin, Y. V. Bakhtiyarova, N. A. Polezhaeva, I. V. Galkina, R. A. Cherkasov, D. B. Krivolapov, A. T. Gubaidullin and I. A. Litvinov, *Russ. J. Gen. Chem.*, 2002, **72**, 384.
35 T. A. Albright, W. J. Freeman and E. E. Schweizer, *J. Org. Chem.*, 1975, **40**, 3437.
36 J. A. Bilbrey, A. H. Kazez, J. Locklin and W. D. Allen, *J. Comput. Chem.*, 2013, **34**, 1189.
37 J. Jover and J. Cirera, *Dalton Trans.*, 2019, **48**, 15036.
38 A. P. Narrainen, S. Pascual and D. M. Haddleton, *J. Polym. Sci., Part A: Polym. Chem.*, 2002, **40**, 439.
39 B. Hammouda, *J. Res. Natl. Inst. Stand. Technol.*, 2013, **118**, 151.
40 C. M. Palmeira, M. I. Rana, C. B. Frederick and K. B. Wallace, *Biochem. Biophys. Res. Commun.*, 2000, **272**, 431.
41 R. C. Bush and R. J. Angelici, *Inorg. Chem.*, 1988, **27**, 681.
42 C. A. Streuli, *Anal. Chem.*, 1960, **32**, 985.